

Organic & Biomolecular Chemistry

This article is part of the

OBC 10th anniversary
themed issue

All articles in this issue will be gathered together
online at

www.rsc.org/OBC10



Cite this: *Org. Biomol. Chem.*, 2012, **10**, 5979

www.rsc.org/obc

PAPER

Combined experimental and theoretical studies on the photophysical properties of cycloparaphenylenes†‡

Yasutomo Segawa, Aiko Fukazawa, Sanae Matsuura, Haruka Omachi, Shigehiro Yamaguchi,* Stephan Irle* and Kenichiro Itami*

Received 26th January 2012, Accepted 28th February 2012

DOI: 10.1039/c2ob25199j

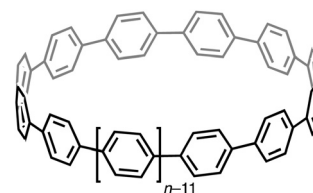
We studied the UV-vis absorption and fluorescence in solution/solid states of $[n]$ cycloparaphenylene ($[n]$ CPP: $n = 9, 12, 14, 15$, and 16), and conducted theoretical studies to better understand the experimental results. The representative experimental findings include (i) the most intense absorption maxima (λ_{abs1}) display remarkably close values (338–339 nm), (ii) the longest-wavelength absorption maxima (λ_{abs2}) are blue-shifted with increasing the ring size (395 → 365 nm), (iii) the emission maxima (λ_{em}) are blue-shifted with increasing the ring size (494 → 438 nm for longest-wavelength maxima), (iv) the fluorescent quantum yields (Φ_{F}) in solution are high (0.73–0.90), (v) the fluorescence lifetimes (τ_{s}) of $[9]$ - and $[12]$ CPP are 10.6 and 2.2 ns, respectively, and (vi) the Φ_{F} values slightly increase in polymer matrix but significantly decrease in the crystalline state. According to TD-DFT calculations, the longest-wavelength absorption (λ_{abs2}) corresponds to a forbidden HOMO → LUMO transition and the most intense absorption (λ_{abs1}) corresponds to degenerate HOMO – 1 → LUMO and HOMO → LUMO + 1 transitions with high oscillator strength. The interesting and counterintuitive optical properties of CPPs (constant λ_{abs1} and blue shift of λ_{abs2}) could be ascribed mainly to the ring-size effect in frontier molecular orbitals (in particular the increase of the HOMO–LUMO gap as the number of benzene rings increases). On the basis of comparative calculations using hypothetical model geometries, we conclude that the unique behavior of HOMO and LUMO of CPPs is due mainly to their lack of a conjugation length dependence in combination with a significant bending effect (particularly to HOMO) and a torsion effect (particularly to LUMO).

Introduction

After many years of efforts,^{1,2} the long-awaited chemical synthesis of cycloparaphenylene (CPP), a simple conjugated carbon nanoring consisting solely of benzene rings with para linkage (Fig. 1), has been accomplished by the groups of Bertozzi *et al.*,³ Itami *et al.*,^{4–8} Yamago *et al.*,^{9,10} and Jasti *et al.*^{3,11} Currently, the modular,⁶ size-selective,^{4,6,9,11} and scalable^{7,8} synthesis of $[n]$ CPPs is possible, and $[12]$ CPP, prepared by the procedure developed in our group, has become commercially available.¹² CPP is an interesting and unique molecular entity not only because of its aesthetic appeal,⁷ unique cyclic and curved conjugation,⁵ photophysical properties,^{3,10,11} and guest-encapsulating properties,^{7,8,13} but also because it represents the

shortest sidewall segment of armchair carbon nanotube structures.^{2,14} Theoretical studies have also uncovered or predicted a number of interesting electronic properties of CPPs.¹⁵ Related to these studies, the groups of Itami *et al.*¹⁶ and Isobe *et al.*¹⁷ recently reported the design and synthesis of short sidewall segments of chiral carbon nanotubes.

The studies on the photophysical properties of CPPs are one of the most important issues for the elucidation of the nature of belt-shaped π -conjugated systems. The groups of Bertozzi/Jasti^{3,11} and Yamago *et al.*^{9,10} independently reported the absorption and fluorescence properties of $[n]$ CPPs. Throughout these works, they demonstrated several features as follows: (1) In the

Fig. 1 Structure of $[n]$ cycloparaphenylene ($[n]$ CPP).

Department of Chemistry, Graduate School of Science, Nagoya University, Chikusa, Nagoya 464-8602, Japan. E-mail:

itami.kenichiro@a.mbox.nagoya-u.ac.jp; Tel: (+81)52-788-6098

† This article is part of the *Organic & Biomolecular Chemistry* 10th Anniversary issue.

‡ Electronic supplementary information (ESI) available: Details of theoretical study. See DOI: 10.1039/c2ob25199j

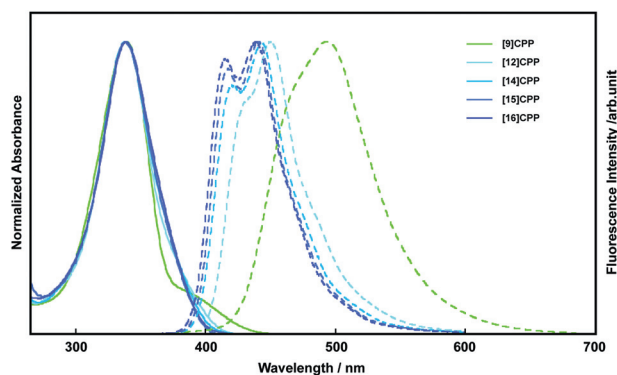


Fig. 2 UV-vis absorption (solid line) and fluorescence spectra (broken line) of [9]-, [12]-, [14]-, [15]-, and [16]CPP in chloroform. Absorption and fluorescence spectra were normalized.

UV-vis absorption spectra, [n]CPPs exhibit intense absorption bands with constant absorption maximum wavelengths (λ_{abs1}) regardless of the ring size. (2) The fluorescence spectra of [n] CPPs are blue-shifted as the number of benzene rings (n) increases. However, the origin of these characteristics has remained unclear. Furthermore, neither fluorescence quantum yields nor solid-state photophysical properties of CPP are reported. Further experimental and theoretical investigations on the photophysical properties of CPPs are eagerly awaited both for the understanding of the nature of belt-shaped π -conjugated systems and for the application of CPPs for light-emitting materials.

Herein we report the novel aspects of the photophysical properties of CPPs. Experimental investigations were carried out for [9]-, [12]-, [14]-, [15]-, and [16]CPP, which are the series of CPPs we have synthesized by the Pd-catalysed modular synthesis⁶ or the nickel-mediated “shotgun” synthesis.^{7,8} In addition to the measurement of CPPs in solution, single crystals of [9]- and [12]CPP were also subjected to the determination of fluorescence properties in the solid state. Theoretical studies on [6]–[20]CPP support prior experiments.

Results and discussion

Absorption and fluorescence properties of [n]CPPs

The electronic absorption and fluorescence properties of [9]-, [12]-, [14]-, [15]-, and [16]CPP in chloroform were thoroughly investigated, including UV-vis absorption, fluorescence spectra, fluorescence quantum yields, and fluorescence lifetimes. The absorption and fluorescence spectra of CPPs are shown in Fig. 2 and the data are summarized in Table 1. The absorption and fluorescence spectra of [14]-, [15]-, and [16]CPP are reported for the first time. In the UV-vis absorption spectra, all CPP derivatives exhibited shoulder-like absorption bands in the long-wavelength region around 400 nm (λ_{abs2}) in addition to the intense absorption bands with the absorption maximum wavelengths (λ_{abs1}) of 338–339 nm. The absorption coefficients (ϵ) were determined to be 1.29×10^5 and $1.58 \times 10^5 \text{ M}^{-1} \text{ cm}^{-1}$ for [9]- and [12]CPP, respectively. In line with the report by Yamago, the ϵ value slightly increases as the ring size of CPP increases.¹⁰

Table 1 Photophysical data for [n]CPPs^a

| Compound | Absorption | | Fluorescence | | |
|----------|--------------------------------|--------------------------------|------------------------------|---------------------|--------------------------|
| | λ_{abs1}^b [nm] | λ_{abs2}^c [nm] | λ_{em}^d [nm] | Φ_{F}^e | τ_{s}^f [ns] |
| [9]CPP | 339 | 395 | 494 | 0.73 | 10.6 |
| [12]CPP | 338 | 378 | 426, 450 | 0.89 | 2.2 |
| [14]CPP | 338 | 369 | 418, 443 | 0.89 | — |
| [15]CPP | 339 | 365 | 416, 440 | 0.90 | — |
| [16]CPP | 339 | 365 | 415, 438 | 0.88 | — |

^a In chloroform. ^b The highest absorption maxima are given. ^c The longest absorption maxima determined by peak separation method are given. ^d Emission maxima and second maxima upon excitation at the absorption maximum wavelengths λ_{abs1} . ^e Absolute fluorescence quantum yields determined by a calibrated integrating sphere system within $\pm 3\%$ errors. ^f Fluorescence lifetimes.

This is in analogy to the case of linear *p*-phenylenes which are well known for increasing molar extinction with increasing chain length due to increasing magnitude of the transition dipole moment.¹⁸ The absorption maximum wavelengths of the shoulder-like absorption bands (λ_{abs2}) were determined by a peak deconvolution program. As shown in Table 1, λ_{abs2} is shifted to shorter wavelength as the ring size increases (395–365 nm) while λ_{abs1} is constant (338–339 nm) regardless of the ring size of CPPs.

All the CPPs showed intense photoluminescence in solution, and their emission colors were dependent of the ring size as already reported.^{3,10} [9]CPP exhibits yellowish-green emission while those of the other CPPs are blue. Thus, the emission maxima in the fluorescence spectra (λ_{em} in Table 1) are blue-shifted with increasing CPP ring size. In the spectra of [14]–[16] CPP, two obvious peaks were observed, whereas the intensities of the shorter-wavelength ones become smaller in the spectra of [9]- and [12]CPP. The shapes of each fluorescence spectrum of all CPPs were identical regardless of the excitation wavelength, indicating that these peaks in emission spectra originated from the same excited state.

The absolute fluorescence quantum yields (Φ_{F}) of CPPs in chloroform were recorded for the first time. All CPPs exhibited high Φ_{F} (0.73–0.90), which are comparable with those of oligo-¹⁹ and poly(*p*-phenylene)s.²⁰ Notably, the Φ_{F} value of [9] CPP was found to be somewhat lower ($\Phi_{\text{F}} = 0.73$) than those of larger-ring congeners [12]- and [14]–[16]CPP ($\Phi_{\text{F}} = 0.88$ –0.90), implying the effect of ring size on the character of excited state. To gain insight into the excited-state dynamics, the time-resolved fluorescence measurements were conducted for [9]- and [12] CPP, and their fluorescence lifetimes (τ_{s}) were determined to be 10.6 and 2.2 ns, respectively. Interestingly, [9]CPP exhibited considerably longer τ_{s} than that of [12]CPP. According to the equations $\Phi_{\text{F}} = k_{\text{r}} \times \tau_{\text{s}}$ and $k_{\text{r}} + k_{\text{nr}} = \tau_{\text{s}}^{-1}$, the radiative (k_{r}) and nonradiative (k_{nr}) decay rate constants from the singlet excited state were determined. The k_{r} value of [12]CPP ($6.9 \times 10^7 \text{ s}^{-1}$) is one-order-of-magnitude higher than that of [9]CPP ($4.0 \times 10^8 \text{ s}^{-1}$). According to classical theory that the radiative rate constant (k_{r}) is related to the oscillator strength (f) and the square of the transition energy,²¹ the greater k_{r} value of [12]CPP should be attributable to the larger oscillator strength (f) of [12]CPP as well as size-independent λ_{abs1} value. On the other hand, the k_{nr}

Table 2 Fluorescence quantum yields of [*n*]CPPs in the solid state^a

| | Crystal | Polymer matrix ^b |
|---------|-------------------|-----------------------------|
| [9]CPP | 0.17 ^c | 0.78 |
| [12]CPP | 0.24 ^d | 0.93 |

^a Absolute fluorescence quantum yields determined by a calibrated integrating sphere system within $\pm 3\%$ errors. ^b 1 wt% in PMMA. ^c Single crystals of [9]CPP·2THF were used. ^d Single crystals of [12]CPP·2(cyclohexane) were used.

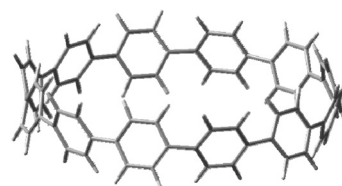
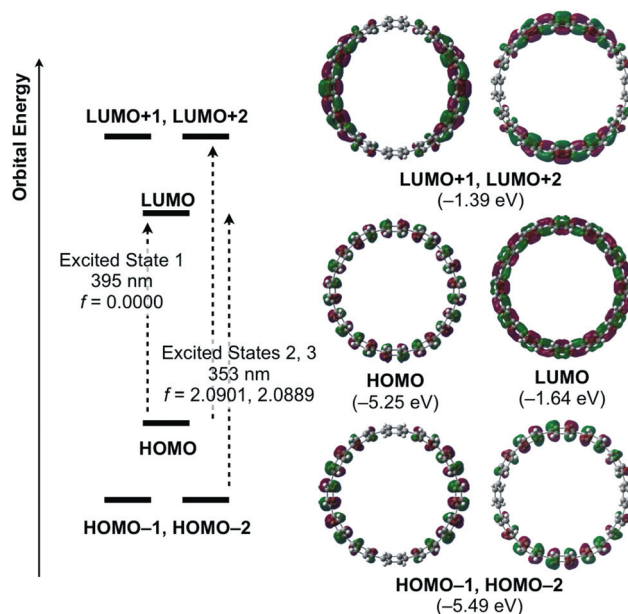
values are comparable each other ($k_{nr} = 2.5 \times 10^7 \text{ s}^{-1}$ and $5.0 \times 10^7 \text{ s}^{-1}$ for [9]- and [12]CPP, respectively).

We then focused our attention on the fluorescence properties of CPPs in the solid state (Table 2). For understanding the relationship between the photophysical properties and the molecular packing structure in the solid state, we studied the photophysical properties of [9]- and [12]CPP, of which solid-state structures were analysed by X-ray crystallography.^{7,8} Both [9]- and [12]CPP adopt herringbone and tubular packing mode in the solid state. Single crystals of [9]CPP·2THF and [12]CPP·2(cyclohexane) were subjected to the measurement of absolute fluorescence quantum yields.²² The Φ_F values of 0.17 and 0.24 for [9]- and [12]CPP, respectively, were found to be significantly lower than those in chloroform. To elucidate the origin of the difference in Φ_F between solution and crystalline state, we evaluated the fluorescence properties in a polymer matrix as a model of diluted solid. The data are also given in Table 2. Both [9]- and [12]CPP, dispersed in a poly(methyl methacrylate) (PMMA) matrix, exhibited intense emissions, and their Φ_F values are slightly higher than those in solution (0.78 for [9]CPP and 0.93 for [12]CPP). These results clearly indicate that the lower Φ_F values of CPPs in crystalline state compared to those in solution are attributable to the intermolecular interaction, which results in the quenching of fluorescence by energy migration and/or self-absorption processes. In line with this assumption, we identified that the shortest intermolecular carbon-carbon distances in the crystal of [9]CPP are *ca.* 3.38 Å, which is almost comparable to the sum of van der Waals radii of carbon atoms (3.40 Å).²³

Assignment of UV-vis absorption

To obtain insight into the photophysical properties especially on the size-dependency of CPP MOs, we performed the DFT calculation of [6]–[20]CPP at the B3LYP²⁴ level of theory with the 6-31G(d) basis set as implemented in the Gaussian 03 program.²⁵ Although only calculations of even-numbered CPPs are shown here owing to the symmetric benefits, odd-numbered CPPs were found to have similar trends. The most stable conformation determined by our previous report⁵ was used for each *n* in [*n*]CPP. As described in Fig. 3, all benzene rings are alternately twisted to form a highly symmetric structure (D_{6d} symmetry for [12]CPP).

First, TD-DFT calculations of [12]CPP were performed at ground state molecular geometries to obtain the information about absorption spectrum of [12]CPP. Depicted in Fig. 4 are the energy diagrams of six frontier molecular orbitals of [12]CPP, from HOMO – 2 to LUMO + 2, and the pictorial representations

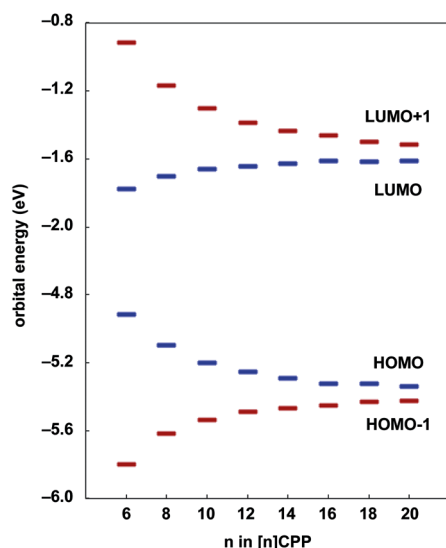
**Fig. 3** Optimized structure of [12]CPP.**Fig. 4** Energy diagrams and pictorial representations of the frontier MOs for [12]CPP, calculated at the B3LYP/6-31G(d) level of theory. Excitation energies were computed by TD-DFT at the same level.

of these six orbitals. The HOMO and LUMO delocalize over the ring of [12]CPP with D_{6d} symmetry, whereas other four orbitals rather delocalize to two opposite sides with C_s symmetry. Degeneracy in energy levels was found for the relevant pairs of frontier orbitals, HOMO – 1/HOMO – 2 (–5.49 eV) and LUMO + 1/LUMO + 2 (–1.39 eV). Throughout this paper, these degenerate orbitals will be described as HOMO – 1 and LUMO + 1 for clarity. Judging from the shape of each orbital, the occupied orbitals represent π and the unoccupied ones represent π^* frontier orbitals of conjugated *p*-phenylenes. According to the TD-DFT calculations, two energetically low-lying characteristic transitions arise from the set of six orbitals: one is a symmetry-forbidden HOMO → LUMO transition with the oscillator strength (*f*) of 0.00 (excited state 1), and the other is a degenerate transition in which both HOMO – 1 → LUMO and HOMO → LUMO + 1 excitations mix with high *f* value of 2.09 (excited states 2 and 3). All of these transitions are π – π^* transitions. Compared with the absorption spectrum of [12]CPP, excited states 2 and 3 should correspond to λ_{abs1} , and the shoulder peak (λ_{abs2}) should be identified with the excited state 1. Deformation away from high symmetry owing to dynamic conformational change may make the forbidden transition possible. For example, the rotation barrier of one benzene ring in [12]CPP was already estimated to be low enough to occur under ambient temperature (3.8 kcal mol^{–1}).⁵

Table 3 TD-DFT vertical one-electron excitations calculated for $[n]$ CPP^a

| Compound | Excitation [nm] | Oscillator strength (f) | Description ^b |
|----------|-----------------|-----------------------------|--------------------------|
| [6]CPP | 491 | 0.00 | H → L |
| | 326 | 0.78 | H - 1 → L, H → L + 1 |
| [8]CPP | 433 | 0.00 | H → L |
| | 339 | 1.31 | H - 1 → L, H → L + 1 |
| [10]CPP | 407 | 0.00 | H → L |
| | 348 | 1.47 | H - 1 → L, H → L + 1 |
| [12]CPP | 395 | 0.00 | H → L |
| | 353 | 2.09 | H - 1 → L, H → L + 1 |
| [14]CPP | 387 | 0.00 | H → L |
| | 356 | 2.53 | H - 1 → L, H → L + 1 |
| [16]CPP | 381 | 0.00 | H → L |
| | 357 | 2.99 | H - 1 → L, H → L + 1 |
| [18]CPP | 381 | 0.00 | H → L |
| | 361 | 3.50 | H - 1 → L, H → L + 1 |
| [20]CPP | 379 | 0.00 | H → L |
| | 362 | 4.01 | H - 1 → L, H → L + 1 |

^a Calculated at the B3LYP/6-31G(d) level. ^b H: HOMO, L: LUMO.

**Fig. 5** Molecular orbital energies for $[n]$ CPP.

Next, the TD-DFT calculations were conducted for other CPPs. For even-numbered CPPs, the shapes of the orbitals and degeneracy features were found to be same as those of [12]CPP. As summarized in Table 3, the transitions of other CPPs were almost identical in nature to those of [12]CPP. The energies of frontier orbitals of CPPs are plotted in Fig. 5. Given the nature and values of these transitions, two characteristics of CPP absorption (constant λ_{abs1} and blue shift of λ_{abs2}) can be understood. As shown in Fig. 5, the HOMO level increases and the LUMO level decreases as the number of benzene ring increases, which is in line with the blue shift of λ_{abs2} (from 491 nm for [6]CPP to 379 nm for [20]CPP). As already mentioned in other theoretical studies of CPPs,^{10,15c,f} this is the reverse of the case of linear *p*-phenylenes. However, the energy of HOMO - 1 increases and the energy of LUMO + 1 decreases as the number of benzene rings increases, similar to the case of linear

Table 4 Length, bending, and torsion effects in HOMO/LUMO energies of CPP

| | | as CPP becomes larger | | |
|--|----------------|-----------------------|------|------|
| | | parameter | HOMO | LUMO |
| | Length Effect | longer | → | → |
| | Bending Effect | less bent | ↓ | ↑ |
| | Torsion Effect | more twisted | ↓ | ↑ |

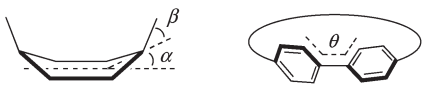
p-phenylenes. Thus, the similarity of energy curves of HOMO - 1/LUMO and HOMO/LUMO + 1 results in similar values of λ_{abs1} regardless of ring size (from 326 nm for [6]CPP to 362 nm for [20]CPP). However, the experimentally observed constant λ_{abs1} values were not reproduced completely by TD-DFT in this case, which we attribute to the fact that the self-interaction error of the TD-B3LYP method increases with system size.

Ring effects on molecular orbitals

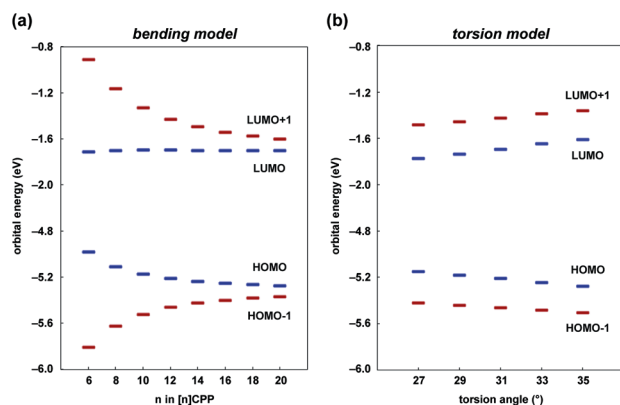
In essence, the above-mentioned interesting and counterintuitive optical properties of CPPs (constant λ_{abs1} and blue shift of λ_{abs2}) can be ascribed mainly to the existence of unique frontier molecular orbitals. Here we propose three factors to explain the behavior of HOMO and LUMO of CPPs; *length effect*, *bending effect*, and *torsion effect* (Table 4). The conjugation effectiveness of linear *p*-phenylenes has been explained or estimated largely by the number of benzene rings (length effect) and the torsion angles of neighboring benzene rings (torsion effect).^{26,27} In the chemistry of strained cyclophane compounds, there also exists the effect of planarity of benzene rings (bending effect).²⁸ Generally the energy of an occupied MO increases and the energy of an unoccupied MO decreases (i) as the number of repeating benzene units increases, (ii) as the torsion angle of neighboring benzene rings decreases, or (iii) as the benzene ring becomes more bent.

Although the energies of most π and π^* MOs of CPP, including HOMO - 1 and LUMO + 1, are affected by these geometrical parameters, it can be anticipated that the influence of length effect is very small or negligible only to HOMO and LUMO because of their “infinite” cyclic conjugation (Fig. 4). In contrast, there should be significant bending and torsion effects in the HOMO/LUMO energies of CPP. The definition and values of bent angles (α and β) and torsion angle θ for CPP are shown in Table 5. For example, if CPP becomes larger, a benzene ring would be less bent, resulting in the stabilization of a π orbital (HOMO) and the destabilization of a π^* orbital (LUMO).²⁸ A torsion angle of neighboring benzene rings becomes larger as the ring size of CPP increases, resulting in the stabilization of HOMO and the destabilization of LUMO because of less overlapping of π -conjugation.²⁷ Thus, both bending and torsion effects lead to the increase of the HOMO–LUMO gap with increasing CPP ring size.

To clarify which of the two effects (bending and torsion) are more significant, we conducted the calculations using

Table 5 Averaged bent angles (α , β ($^\circ$)) and torsion angles (θ ($^\circ$)) in $[n]$ CPP^a


| n in $[n]$ CPP | 6 | 8 | 10 | 12 | 14 | 16 | 18 | 20 |
|------------------------|------|------|------|------|------|------|------|------|
| Bent angle α | 12.5 | 9.3 | 7.3 | 6.1 | 5.2 | 4.6 | 4.0 | 3.6 |
| Bent angle β | 18.0 | 13.7 | 11.1 | 9.3 | 8.0 | 6.9 | 6.3 | 5.6 |
| Torsion angle θ | 27.4 | 30.7 | 32.7 | 33.4 | 34.4 | 35.0 | 34.9 | 35.1 |

^a Optimized at B3LYP/6-31G(d) level.**Fig. 6** (a) Molecular orbital energies for $[n]$ CPP. All torsion angles (θ) are restricted to 31° . (b) Molecular orbital energies for $[12]$ CPP. All torsion angles (θ) are restricted to 27° , 29° , 31° , 33° , and 35° .

hypothetical model geometries for $[n]$ CPPs. Shown in Fig. 6(a) are the molecular orbital energies of “bending model” CPP in which all torsion angles (θ) are restricted to 31° . Even though torsion angles are all fixed, the resulting plot was similar to that for optimized CPP shown in Fig. 5. Fig. 6(b) shows the MO energies of “torsion model” CPPs, where $[12]$ CPP was optimized with several restricted torsion angles. The bent angles of these $[12]$ CPPs are constant in the range of 27° – 35° , which correspond to the torsion angles in optimized $[6]$ – $[20]$ CPP (Table 5). The most noticeable difference between Fig. 6(a) and 5 is that the LUMO level becomes more flat in the range from $[6]$ - to $[20]$ CPP, indicating its stronger sensitivity towards torsion, while the HOMO level behavior is almost unchanged. It is clear from Fig. 6(b) that the torsion effect is a main contributor for the unique behavior of LUMO energies, and that bending seems less important for this MO. The torsion effect does also have an influence for the unique behavior of HOMO energies, but likely not as a main contributor. This finding can be rationalized by the bonding nature of HOMO and LUMO. While the HOMO is mainly localized within individual phenylene units and thereby rather independent from the inter-ring angle, the LUMO is a π -bond mainly localized on the C–C bonds connecting two phenylene units, and therefore strongly affected by the p-orbital alignment between the two carbon atoms. The HOMO, on the other hand, experiences increasingly antibonding interactions between orbital lobes on neighboring phenylene units with increasing bending angle.

On the basis of these control calculations, we conclude that the unique behavior of HOMO and LUMO of CPPs is due mainly to the lack of a conjugation length energy dependence in the HOMO and LUMO and the significant influence of bending and torsion effects on orbital energies. The bending effect is more pronounced in HOMO energies, whereas the LUMO energies are more affected by the torsion angles of neighboring benzene rings.

Conclusion

In summary, we studied the UV-vis absorption and fluorescence in solution/solid states of $[n]$ CPP ($n = 9, 12, 14, 15$, and 16), and conducted theoretical studies to better understand the experimental results. The representative experimental findings include (i) the most intense absorption maxima (λ_{abs1}) display remarkably close values (338 – 339 nm), (ii) the longest-wavelength absorption maxima (λ_{abs2}) are blue-shifted with increasing the ring size ($395 \rightarrow 365$ nm), (iii) the emission maxima (λ_{em}) are blue-shifted with increasing the ring size ($494 \rightarrow 438$ nm for longest-wavelength maxima), (iv) the fluorescent quantum yields (Φ_{F}) in solution are high (0.73 – 0.90), (v) the fluorescence lifetimes (τ_{s}) of $[9]$ - and $[12]$ CPP are 10.6 and 2.2 ns, respectively, and (vi) the Φ_{F} values slightly increase in polymer matrix but significantly decrease in the crystalline state. According to TD-DFT calculations, λ_{abs2} corresponds to a forbidden HOMO \rightarrow LUMO transition and λ_{abs1} corresponds to degenerate HOMO $- 1 \rightarrow$ LUMO and HOMO \rightarrow LUMO $+ 1$ transitions with high oscillator strength. The interesting and counterintuitive optical properties of CPPs (constant λ_{abs1} and blue shift of λ_{abs2}) could be ascribed mainly to the ring-size effect in frontier molecular orbitals (in particular the increase of the HOMO–LUMO gap as the number of benzene rings increases). On the basis of comparative calculations using hypothetical model geometries, we conclude that the unique behavior of HOMO and LUMO of CPPs is due mainly to their lack of a conjugation length dependence in combination with a significant bending effect (particularly to HOMO) and a torsion effect (particularly to LUMO). The questions remaining unanswered include (i) the dual emission and (ii) the blue-shift tendency in fluorescence. The theoretical investigation for these questions will be reported in due course. We believe that the ring effect uncovered in this study may find uses in the emerging field of organic electronics.

Experimental section

Photophysical property measurements

UV-vis absorption spectra were recorded on a Shimadzu UV-3510 spectrometer with a resolution of 0.5 nm. Emission spectra were measured with an F-4500 Hitachi spectrometer with a resolution of 0.2 nm. Dilute solutions in degassed spectral grade chloroform in a 1 cm square quartz cell were used for measurements. Absolute fluorescence quantum yields were determined with a Hamamatsu C9920-02 calibrated integrating sphere system equipped with multichannel spectrometer (PMA-11). Fluorescence lifetimes were measured with a Hamamatsu Picosecond Fluorescence Measurement System C4780

equipped with a USHO pulsed nitrogen laser (excitation wavelength 337 nm with a repetition rate of 10 Hz).

Computational method

The geometry optimizations and time-dependent (TD) DFT calculations of all compounds were performed using the B3LYP theory and 6-31G(d) basis set as implemented in the Gaussian 03 program. The details are shown in the ESI.†

Acknowledgements

This work was supported by the Funding Program for Next Generation World-Leading Researchers from JSPS (220GR049 to K. I.). We thank Mr. Kazuhiko Nagura for assistance in the analysis of UV-vis spectra by peak deconvolution program. Calculations were performed using the resources of the Research Center for Computational Science, Okazaki, Japan.

Notes and references

- Representative attempts: (a) V. C. Parekh and P. C. Guha, *J. Indian Chem. Soc.*, 1934, **11**, 95; (b) R. Friederich, M. Nieger and F. Vögtle, *Chem. Ber.*, 1993, **126**, 1723.
- Reviews: (a) M. Iyoda, J. Yamakawa and M. J. Rahman, *Angew. Chem., Int. Ed.*, 2011, **50**, 10522; (b) T. Kawase and H. Kurata, *Chem. Rev.*, 2006, **106**, 5250; (c) B. D. Steinberg and L. T. Scott, *Angew. Chem., Int. Ed.*, 2009, **48**, 5400; (d) G. J. Bodwell, *Nat. Nanotechnol.*, 2010, **5**, 103; (e) R. Jasti and C. R. Bertozzi, *Chem. Phys. Lett.*, 2010, **494**, 1.
- Synthesis of [9]-, [12]-, and [18]CPP: R. Jasti, J. Bhattacharjee, J. B. Neaton and C. R. Bertozzi, *J. Am. Chem. Soc.*, 2008, **130**, 17646.
- Selective synthesis of [12]CPP: H. Takaba, H. Omachi, Y. Yamamoto, J. Bouffard and K. Itami, *Angew. Chem., Int. Ed.*, 2009, **48**, 6112.
- Y. Segawa, H. Omachi and K. Itami, *Org. Lett.*, 2010, **12**, 2262.
- Modular and size-selective synthesis of [14]-, [15]-, and [16]CPP: H. Omachi, S. Matsuura, Y. Segawa and K. Itami, *Angew. Chem., Int. Ed.*, 2010, **49**, 10202.
- Concise synthesis and crystal structure of [12]CPP: Y. Segawa, S. Miyamoto, H. Omachi, S. Matsuura, P. Šenel, T. Sasamori, N. Tokitoh and K. Itami, *Angew. Chem., Int. Ed.*, 2011, **50**, 3244.
- Concise synthesis and crystal structure of [9]CPP: Y. Segawa, P. Šenel, S. Matsuura, H. Omachi and K. Itami, *Chem. Lett.*, 2011, **40**, 423.
- Selective synthesis of [8]CPP: S. Yamago, Y. Watanabe and T. Iwamoto, *Angew. Chem., Int. Ed.*, 2010, **49**, 757.
- Random synthesis of [8]-[13]CPP: T. Iwamoto, Y. Watanabe, Y.-I. Sakamoto, T. Suzuki and S. Yamago, *J. Am. Chem. Soc.*, 2011, **133**, 8354.
- Synthesis of [7]CPP: T. J. Sisto, M. R. Golder, E. S. Hirst and R. Jasti, *J. Am. Chem. Soc.*, 2011, **133**, 15800.
- [12]CPP is now commercially available from Tokyo Chemical Industry Co., Ltd (TCI), catalog no. C2449.
- T. Iwamoto, Y. Watanabe, T. Sadahiro, T. Haino and S. Yamago, *Angew. Chem., Int. Ed.*, 2011, **50**, 8342.
- Previous reports on the synthesis of fully conjugated macrocycles related to CPPs: Picotubes: (a) S. Kammermeier and R. Herges, *Angew. Chem., Int. Ed. Engl.*, 1996, **35**, 417; (b) S. Kammermeier, P. G. Jones and R. Herges, *Angew. Chem., Int. Ed. Engl.*, 1997, **36**, 2200; (c) T. Tsuji, M. Okuyama, M. Ohkita, T. Imai and T. Suzuki, *Chem. Commun.*, 1997, 2151. Cyclothiophenes: (d) J. Krömer, I. Rios-Carreras, G. Fuhrmann, C. Musch, M. Wunderlin, T. Debaerdemaeker, E. Mena-Osteritz and P. Bäuerle, *Angew. Chem., Int. Ed.*, 2000, **39**, 3481; (e) F. Zhang, G. Götz, H. D. F. Winkler, C. A. Schalley and P. Bäuerle, *Angew. Chem., Int. Ed.*, 2009, **48**, 6632. Cyclopyrroles: (f) D. Seidel, V. Lynch and J. L. Sessler, *Angew. Chem., Int. Ed.*, 2002, **41**, 1422; (g) T. Köhler, D. Seidel, V. Lynch, F. O. Arp, Z. Ou, K. M. Kadish and J. L. Sessler, *J. Am. Chem. Soc.*, 2003, **125**, 6872. Cyclocarbazoles: (h) S.-H. Jung, W. Pisula, A. Rouhanipour, H. J. Räder, J. Jacob and K. Müllen, *Angew. Chem., Int. Ed.*, 2006, **45**, 4685. Acetylene-inserted CPPs: (i) T. Kawase, H. R. Darabi and M. Oda, *Angew. Chem., Int. Ed. Engl.*, 1996, **35**, 2664; (j) M. Srinivasan, S. Sankararaman, H. Hopf and B. Varghese, *Eur. J. Org. Chem.*, 2003, 660.
- Theoretical studies of CPPs: (a) Ref. 5 (b) K. Tahara and Y. Tobe, *Chem. Rev.*, 2006, **106**, 5274; (c) M. N. Jagadeesh, A. Makur and J. Chandrasekhar, *J. Mol. Model.*, 2000, **6**, 226; (d) S. Basu, P. Ghosh and B. Mandal, *Mol. Phys.*, 2008, **106**, 2507; (e) B. M. Wong, *J. Phys. Chem. C*, 2009, **113**, 21921; (f) D. Sundholm, S. Taubert and F. Pichierri, *Phys. Chem. Chem. Phys.*, 2010, **12**, 2751; (g) S. Taubert, D. Sundholm and F. Pichierri, *J. Org. Chem.*, 2010, **75**, 5867; (h) S. M. Bachrach and D. Stück, *J. Org. Chem.*, 2010, **75**, 6595.
- Synthesis of [13]cycloparaphenylene-2,7-naphthylene as a sidewall segment of [15,14]CNT: H. Omachi, Y. Segawa and K. Itami, *Org. Lett.*, 2011, **13**, 2480.
- Synthesis of [4]cyclochrysene as sidewall segments of [12,8]-, [11,9]-, and [10,10]CNT: S. Hitosugi, W. Nakanishi, T. Yamasaki and H. Isobe, *Nat. Commun.*, 2011, **2**, 492.
- Molecular Photonics, Kodansha*, ed. K. Horie, H. Ushiki and F. M. Winnik, John Wiley & Sons, Inc., Weinheim and Chichester, Tokyo, 2000, p. 48.
- R. Katoh, K. Suzuki, A. Furube, M. Kotani and K. Tokumaru, *J. Phys. Chem. C*, 2009, **113**, 2961.
- M. Banerjee, R. Shukla and R. Rathore, *J. Am. Chem. Soc.*, 2009, **131**, 1780.
- N. J. Turro, *Modern Molecular Photochemistry*, University Science Books, Sausalito, 1991.
- Katoh and coworkers demonstrated that fluorescence quantum yields of oligo(*p*-phenylene)s in crystalline state are highly affected by the crystalline size and/or the defect of crystals by mechanical milling process (see ref. 19). Regarding these issues, the single crystals of [9]- and [12]CPP were subjected to the measurements without any milling process.
- Intramolecular C–C distance of ca. 2.6 Å in [12]CPP has a large margin of error because correspondent carbon atoms are parts of a disordered moiety.
- (a) A. D. Becke, *J. Chem. Phys.*, 1993, **98**, 5648; (b) C. Lee, W. Yang and R. G. Parr, *Phys. Rev. B*, 1988, **37**, 785; (c) P. J. Stephens, F. J. Devlin, C. F. Chabalowski and M. J. Frisch, *J. Phys. Chem.*, 1994, **98**, 11623.
- M. J. Frisch, *et al.*, *GAUSSIAN 03 (Revision E.01)*, Gaussian, Inc., Wallingford, CT, 2004. See the ESI† for full reference.
- R. E. Martin and F. Diederich, *Angew. Chem., Int. Ed.*, 1999, **38**, 1350.
- (a) V. Lukeš, R. Šolc, M. Barbatti, M. Elstner, H. Lischka and H.-F. Kauffmann, *J. Chem. Phys.*, 2008, **129**, 164905; (b) A. Karpfen, C. H. Choi and M. Kertesz, *J. Phys. Chem. A*, 1997, **101**, 7426.
- (a) S. Grimme, *J. Am. Chem. Soc.*, 1992, **114**, 10542; (b) T. Tsuji, M. Ohkita and H. Kawai, *Bull. Chem. Soc. Jpn.*, 2003, **75**, 415; (c) B. L. Merner, L. N. Dawe and G. J. Bodwell, *Angew. Chem., Int. Ed.*, 2009, **48**, 5487.